A Simplified Balloon Payload

For Stratospheric Conductivity Measurements

A Senior Honors Thesis Presented to the

Faculty of the Department of Physics

University of Houston

In Partial Fulfillment of the

Requirements for the Degree of Bachelor of Science

By Alexandra Rae Briggs Ulinski

May 2022

A SIMPLIFIED BALLOON PAYLOAD

FOR STRATOSPHERIC CONDUCTIVITY MEASUREMENTS

____

Alexandra Rae Briggs Ulinski

APPROVED:

____

Dr. Edgar Bering III

Department of Physics

____

Dr. Rebecca Forrest

Department of Physics

____

Dr. Donna Stokes

Department of Physics

____

Dr. Dan E. Wells, Dean

College of Natural Sciences and Mathematics

ACKNOWLEDGEMENTS

I would like to acknowledge Dr. Edgar Bering III for his dedication to helping me succeed in creating this payload design, and for sharing the designs and experiences from his own research on atmospheric conductivity. His insight was invaluable. I would also like to appreciate the undergraduate students in the USIP IV program that contributed to the design, testing, parts shopping, and construction of this payload. I would especially like to thank Rachel Nathan, Elizabeth Hernandez, Andy Nguyencuu, and Carlos Salas for their amazing work on this challenging project. My USIP family has been a wonderful source of support, fun, and frustration, as any great family would be.

A Simplified Balloon Payload

For Stratospheric Conductivity Measurements

An Abstract of a Senior Honors Thesis

Presented to the Faculty of the

Department of Physics

University of Houston

In Partial Fulfillment of the

Requirements for the Degree of Bachelor of Science

By Alexandra Rae Briggs Ulinski

May 2022

ABSTRACT

There are still many open questions about the Earth's atmosphere, and to answer them scientists need data from experimental observations. Stratospheric conductivity measurements are a vital component of global electric circuit research; however, in the twenty-first century there have been very few experiments designed to advance this area of research or investigate puzzling observations made in the decades before. To address this deficiency, this thesis aimed to design a lightweight, low-cost, balloon instrument that could measure stratospheric conductivity. The goal was to create a design that could be shared and replicated by other student groups, adding fresh experimental observations to the available data; thus, allowing scientists to improve models, explain anomalies, and explore new applications of this knowledge. To design an effective, yet simple instrument, previous balloon payloads were analyzed and modified to reduce complexity, weight, and cost. The design, consisting of two spherical conducting probes separated horizontally by a high resistivity boom was shared via ConductivityResearch.com. A prototype was constructed, weighing only 2.72 kg (not including flight train and telemetry devices), and costing just under $2000 (including balloon, helium, and flight train). Initial tests suggest that the design will be capable of measuring atmospheric conductivity and can be replicated with relative ease. The prototype will soon be fully tested during a balloon campaign in Alaska.

TABLE OF CONTENTS

List of Tables

List of Figures

1 Introduction

The continuous current that flows between the ionosphere and the Earth's surface is a central element of atmospheric physics and meteorology. Changes in this global electric circuit can be indicative of global weather patterns, space weather events, and pollution levels; thus, measurements of various aspects of the Earth's electrical atmosphere were collected for decades. However, there are still many unanswered questions about the air above us. For example, variations in stratospheric conductivity were measured repeatedly in past experiments, but many of the short-term fluctuations remain unexplained [1, 2, 3]. The failure of our models to predict or clarify the findings suggests that we are misunderstanding something about our atmosphere. Addressing this gap in scientific knowledge could help advance our ability to predict weather, understand climate changes, and monitor air pollution [4, 5, 6]. Despite this, there have been relatively few attempts to measure stratospheric electrical properties in recent decades [7]. Therefore, the primary objective of this thesis was to provide and discuss a design for a low-cost, lightweight instrument that can measure stratospheric conductivity. The secondary objective was to assess the feasibility for replication by other college, or even high school, student groups. The overarching goal for this research was to create a design that is affordable, simple, and effective enough to be reproduced by many others so that plentiful new data can be made available to researchers attempting to better understand the global electric circuit.

1.1 Introduction to Conductivity

Stratospheric conductivity is a measure of how easily charged particles can move through the atmosphere. It is a fundamental property of the air and a central component of global electric circuit studies. The circuit is linked to global temperatures and weather events such as thunderstorms, and a more complete model can provide insight into storm and overall climate behavior. Changes in the conductivity are also indicative of other atmospheric conditions. For example, aerosols reduce atmospheric conductivity, so researchers have used conductivity measurements to infer tropospheric and stratospheric air pollution levels [8, 5, 4]. Conductivity also plays a role in electromagnetic wave propagation [9], which is vital to the study of space weather [10], communications, remote-sensing, and detecting the warning signs of earthquakes [11, 12].

Atmospheric conductivity, σ, is proportional to the product of ion concentration, n, and ion mobility, as shown by the equation

$$\sigma = ne(\mu^{+} + \mu^{-}) \,, \tag{1}$$

where positive and negative ion concentrations are assumed equal, e is the elementary charge, and μ^{+} and μ^{-} are positive and negative ion mobilities [2]. Conductivity has been shown experimentally to increase exponentially (see Figure 1) with altitude due to greater exposure to radiation from space, combined with the increased mobility that comes with less dense air [1]. Near sea level, atmospheric conductivity is typically on the order of magnitude of 10^{-13} or 10^{-14} $(\Omega \cdot m)^{-1}$, whereas 10^{-11} $(\Omega \cdot m)^{-1}$can be expected at altitudes of about 32 km [13, 15].

1.2 Motivation for study

The charged particles that make up the electric current in the air are primarily ions formed by cosmic radiation. Therefore, as conductivity is proportional to the product of ion concentration and ion mobility, global conductivity models have relied heavily on average cosmic ray flux at various latitudes [1]. This foundational relationship adequately explains observations of lower conductivity at lower latitudes compared to near the poles. The Earth's magnetic field offers the greatest radiation shielding near the equator, so there are fewer ions at lower latitudes [3]. However, models based primarily on cosmic rays have failed to consistently predict actual conductivity values.

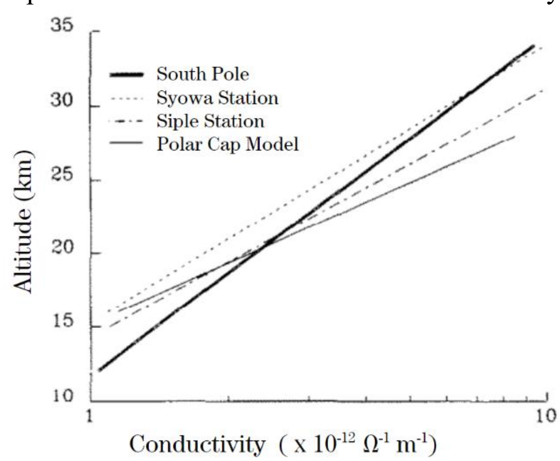

Figure 1: Exponential increase in stratospheric conductivity. The exponential relationship was observed during campaigns at the South Pole, Syowa Station, and Siple Station. Figure adapted from Byrne, Benbrook & Bering (1991) [1].

Furthermore, they have no ability to explain the many temporal and spatial variations that have been recorded spanning decades [1, 14]. And while models have improved throughout the years, we are still left with many unanswered questions [2].

Variations occurring on time scales of weeks to months have been attributed to changes in local cosmic ray flux, aerosol injections, and geomagnetic storms. On the other hand, short-term variations—on the scale of minutes to hours—have not been adequately explained [1, 3, 15]. With further study under a variety of conditions it may be possible to determine the causes for these short-term variations and improve conductivity models. Furthermore, a better understanding of the link between conductivity and other environmental factors may lead scientists to find ways to use conductivity measurements to study other atmospheric features, such as pollution levels, cloud formation, global storm activity and average global temperatures. There may also be potential to use conductivity instruments as predictive weather tools. However, without new stratospheric data, that potential will not be realized, and the electrical anomalies will endure as unanswered questions.

While there are several factors contributing to the lack of recent research involving atmospheric conductivity, one problem is that for research to be significant and for models to be improved, a great deal of measurements are required—across many locations and times, and under different conditions. Completing all these measurements would be a monumental task for a single research group. A solution to this problem is to have many people throughout the world contribute to a global database that can be analyzed by any scientists wishing to further the research. Though, while creating the database is well within the capability of the scientific community, we will still lack the actual measurements if we continue with the status quo. I suggest that the critical issues are that there are cost and complexity barriers for prospective researchers that would otherwise be capable of contributing. Global electric circuit research payloads can cost tens of thousands of dollars and weigh hundreds of kilograms. To limit these barriers, I aimed to develop an instrument that would be as lightweight and low-cost as possible, while maintaining data quality. It is my hope that sharing this design with high school and college student groups will encourage them to make their own measurements, increasing the available conductivity data while encouraging the youth to get involved in scientific research.

1.3 Experimental Overview

To begin the design process for an atmospheric electricity investigation, I encouraged a team of four other students within the University of Houston extension of the Undergraduate Student Instrument Project (USIP IV) to begin work with me on the instrument, starting in January of 2020. I directed the literature review where we learned about the science of atmospheric conductivity and assessed the designs of previous researchers, including my thesis director, Dr. Edgar Bering III. As we reviewed designs from prior experiments, I decided on what elements I could remove to simplify the design while still making measurements that would be valuable for our overarching goals. By focusing solely on stratospheric conductivity and a few additional environmental measurements, I was able to reduce the cost of instrument to fit into our $3,000 budget and reduce the weight to fit the 2.72 kg mass budget. I finalized much of the design, consisting of two spherical conducting probes, separated horizontally by a high resistivity boom, in September 2021 upon passing the Critical Design Review. Construction of the balloon-borne instrument began in 2021, culminating in a prototype that was used to test the effectiveness of the design.

2 Background

Variations in conductivity are a result of changes in either the ion density, or ion mobility. The complication lies in the fact there are many sources of variation for these two parameters. While some sources, such as the latitude gradient, have been accounted for by cosmic ray flux, other fluctuations cannot be so easily explained.

As scientists sought to improve agreement between theory and experiment, factors such as aerosol concentration and latitudinal temperature changes helped to better align observed data with conductivity models [4]. It was also proposed that spatial variations may be due to aerosols, gravity waves, or cloud variations, because these factors influence the structure and concentration of ionized particles. Ions bind to aerosol particles, decreasing ion mobility and thus decreasing conductivity (though only to a point). Aerosols also affect cloud variation by providing a basis for condensation [7]. Cloud variation contributes to conductivity, in part, by affecting high energy particles. The relationship between high energy ion currents and electrical conductivity in the clouds can be investigated by observing and quantifying data on cloud condensation nuclei. Additionally, gravity waves were considered in new models because internal gravity waves can induce variations in electrical conductivity spatially. When they break at the troposphere, they release energy into the upper layers of the atmosphere, which alters electron density at heights where very low frequency (VLF) waves are reflected [6]. Thus, evidence of gravity waves affecting electrical conductivity can be seen in altered amplitude and phase of VLF narrow band signals that make it to the lower layers of the atmosphere. Geomagnetic wave events have also been suggested to correlate with conductivity variations. The unusual doubling of the conductivity observed during a geomagnetic wave event by Bering et al (2005) suggested a correlation between x-ray precipitation and conductivity, but further experimentation and observations are required to expand upon this possibility [15]. The common theme in all these relationships is that more data is needed to explain them thoroughly, which provides motivation to perform further research on atmospheric conductivity.

Variations with time scales of minutes to days can have amplitudes of a factor of 2 or more have been the most difficult to account for. Furthermore, there seems to be a gradient to the variations themselves. At high magnetic latitude, variations increase, and the cause remains a mystery. This enigma is problematic, not simply because it reflects a lack of understanding, but also because the variations obscure any long-term climatic trends in conductivity [3]. With recent advances, we are getting closer to being able to use conductivity models to simulate and analyze the effects of events such as volcanic eruptions and nuclear explosions. However, science relies on experiments to verify the accuracy of their models [2].

3 Methodology

The goal of developing a simplified, sharable stratospheric conductivity instrument was achieved in four main phases: Discovery, design, construction, and testing and assessment.

3.1 Discovery

The first phase of this project was kicked off by a series of lectures throughout Spring 2020 given by various University of Houston professors and guest speakers with experience in research at other organizations. As I developed my ideas about what I wanted to measure, these lectures helped me formulate specific science questions and sift through what measurements would be scientifically interesting and achievable. That May, my team and I collaboratively wrote our first essay identifying our questions, and the measurements we would make to answer them. Although much changed after that essay was written, it was a critical part of the process. The act of writing forces one to organize thoughts and reflect on plans and assumptions. As a result, I had a clearer idea of what needed to be accomplished and the restrictions that I would operate within.

The experiment had the following primary constraints: The first was weight. The payload could not weigh more than 2.72 kg (6 lbs.) due to Federal Aviation Administration (FAA) regulations (Subchapter F, Part 101) and the limitations of the 2000 g latex weather balloons that all USIP IV projects would use. The second constraint was cost. The payload, including spare parts and copies, could not cost more than $3,000. This limit was determined from both the USIP project budget, and the fact that if the payload was too expensive to build, it would be less feasible for other researchers to replicate. The third requirement was simplicity. The payload needed to be simple enough for student groups at either the advanced high school or college undergraduate levels to replicate. That meant minimal use of specialized equipment and supplies. That is not to say that resources were limited to only what is available in a standard home garage; some scientific research supplies and equipment would be needed. The idea though, was to keep the design as simple as possible to maximize the accessibility of this research.

3.2 Design

The following summer was spent analyzing the pros and cons of previous conductivity instruments, keeping in mind the requirements that we set for ours. Due to the COVID-19 pandemic, the design process was extended into 2021 as the situation significantly disrupted collaborative work on the project. However, steady progress continued, and my team and I used design tools such as TinkerCAD to make simple models of the payload that were easily shareable and could be modified by any member of the team. TinkerCAD was particularly useful because it was free, web-based, and easy to learn—even for people that have no experience using computer-aided design (CAD) software.

The design work for this thesis was completed primarily within the Conductivity team that I lead. However, it is noteworthy that the Conductivity team is just one sub-team of USIP IV. There are five Systems teams within the larger project that provide support for certain aspects of the science payloads. Consequently, the Conductivity team received input from the Power, Structures, Telemetry, Avionics, and Flight Ops teams. All Systems teams are made up of members that are also on at least one science team so there are many overlapping responsibilities. Therefore, when I organized the Conductivity team into focus areas during the design phase, I took advantage of team-member Systems specialties. Physics major Rachel Nathan handled the power systems and the structure of the payload box in collaboration with the Power and Structures Systems Teams. I chose her for this role since she is a member of the Power team and the lead of the Structures team. Andy Nguyencuu leads the Telemetry team and is a computer science major, so I assigned him to work on the code for the payload and ensure our telemetry could be transmitted. Computer engineering major Elizabeth Hernandez is the Project Director for USIP IV and leads the Frequencies science team. She assisted me with the circuit design. I tasked physics major Adrian Rangel to assist me with parts acquisition and prototyping. I led the Conductivity team meetings at least once per week throughout the design phase to exchange updates, review work done, and assign new tasks. I used Smartsheet software to maintain a Gantt chart so that I could manage tasks and deadlines efficiently.

When the design was well underway, and team members were able to work on their tasks with less input from me, I shifted my focus to the design of the circuit required to make the conductivity measurements. I used NI Multisim to design a schematic based on an existing circuit that Dr. Bering had used successfully in past experiments. I altered the circuit to make it smaller and simpler, offloading some of the functions to an Arduino microprocessor and updating some of the components. To make the board layout, I used NI Ultiboard.

3.3 Construction

To ensure that the initial design could be shared and used effectively, the construction phase began in early 2021. This phase was also slowed considerably by the pandemic since concurrent physical presence in the lab was required, yet difficult to achieve. Additionally, one team member left the project after graduating in May of 2021. However, physics major Carlos Salas joined the team the following summer and helped the team continue construction with renewed vigor.

Although some parts and materials were available in the laboratory already, many parts were ordered from a variety of distributors and manufacturers so that construction could be completed. Thorough planning and early shopping were essential because some parts had long lead times or were unexpectedly difficult to acquire. All construction took place in the USIP labs in Science and Research 1, rooms 528 and 532, except for the printed circuit board. The complete board layout was printed by OSHPark. However, the Conductivity team and I were responsible for all soldering of the components which were ordered separately.

3.4 Testing and Assessment

The final step was to ensure that the payload design met all requirements by testing the prototype and reviewing the design. Preliminary testing was conducted to provide confidence that the primary goal of the instrument—measuring atmospheric conductivity—could be met. Potential was applied to the probes with a power supply. Then, the probe surfaces were checked with a digital multimeter to make sure that voltage was applied evenly across the spherical probes. Additionally, electrical connectivity tests were performed on all cables and connections. Environmental sensor outputs were tested, and extensive testing was conducted on the payload box to evaluate insulation and structural integrity.

To address the cost of the payload, it was necessary to examine not only the money that was spent on this thesis, but also what would be spent by a group that had none of the materials and parts to start with. Since this project had access to laboratories that had completed similar experiments in the past, many purchases were unnecessary. On the other hand, this project also spent extra money on redundant parts for copies that are anticipated to launch on multiple flights in the future. Therefore, a separate budget sheet was created to show what a new research group could expect to spend on a single copy of this instrument. The payload prototype was weighed to make sure the payload will comply with weight regulations. Simplicity is somewhat more difficult to assess until the design is actually shared and replicated. However, the clarity of instructions, tools and equipment required for construction, and complexity of fabrication and measurement methods were all considered when evaluating the completed design.

4 Implementation of the Design Process

The implementation of the design process will be described in the following section to provide justification for design decisions. Moreover, a more thorough explanation of the work completed during this thesis will be put forth.

4.1 Measurement Technique Selection

The method by which we would make conductivity measurements was one of the early decisions to be made since the entire experimental design had to fit the technique to be used. Repeated experiments have shown that a technique known as the relaxation time method is an effective way to measure stratospheric conductivity [16, 7]. This technique, described in further detail by Byrne et al. (1990) [17], uses two or more probes attached to a balloon payload to measure the conductivity. The probes are charged to opposite potentials—one probe positive and one probe negative. The probes are then allowed to relax back to zero with respect to the surroundings by movement of ions in the air. The time step, τ, of the decaying potential is inversely proportional to the conductivity, σ, by

$$\sigma = \frac{\epsilon_0}{\tau}, \tag{2}$$

where ϵ_0 is the permiativity of free space, approximated to 8.854×10^{-12} F·m^{-1} [18]. Since we had a wealth of information available on the relaxation time method, and the instrumentation required seemed to be achievable with our budget, I proceeded to design around this method.

Many designs from past experiments used six probes, arranged as in figure 1. With six probes, and a rotation motor, these payloads were able to measure multiple parameters, often including vertical and horizontal conductivity, electric fields, x-ray precipitation, and conduction currents. They were also equipped with a variety of other sensors to measure quantities such as ambient temperature, pressure, and humidity [1, 7].

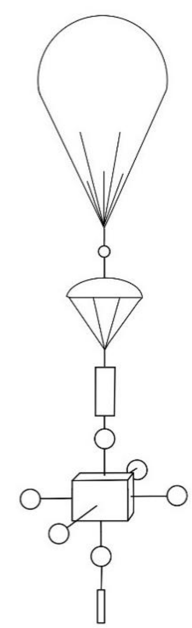

Figure 2: Generalized design outline of balloon instruments used in past atmospheric electricity experiments. It was common for six probes to be used, accompanied by other equipment such as x-ray scintillators and communication devices.

While these instruments provided a wealth of data on the electrical environment, there were several qualities of the designs that made it impractical for this research. The first is weight; the balloon payloads reviewed weighed between 24 and 500 kg [1]. Due to the limitations of the 2000g latex weather balloon, and FAA regulations, our payload could not exceed 2.72 kg. The designs also far exceeded the budget requirements for this instrument. Furthermore, since the goal of this work is to encourage greater participation in this area of research, it was necessary to limit the complexity of the design as much as possible. As such, the instrument designed for this research uses only two spherical probes, oriented horizontally; though, a vertical orientation can be easily achieved with slight modifications. The probes are separated by a boom made from a carbon-fiber tube. With this design, the relaxation time method can be employed to measure the conductivity.

4.2 Instrumentation Development

4.2.1 Probes

With the basic design and measurement technique decided, the details of the instrument were further developed. The two probes would be made from craft foam spheres, 30 cm in diameter. The spheres would be coated in a colloidal carbon suspension called Aquadag to make them conductive on the surface. A small brass plate, approximately 2.5 cm by 2.5 cm, would be attached to each sphere using RTV 102 glue. A nut would be soldered to the back of each plate and a bolt threaded through to attach the coax cables that would apply voltage to the probes. The probe plate assembly is shown in figure 3. The boom would run through the center of the probes.

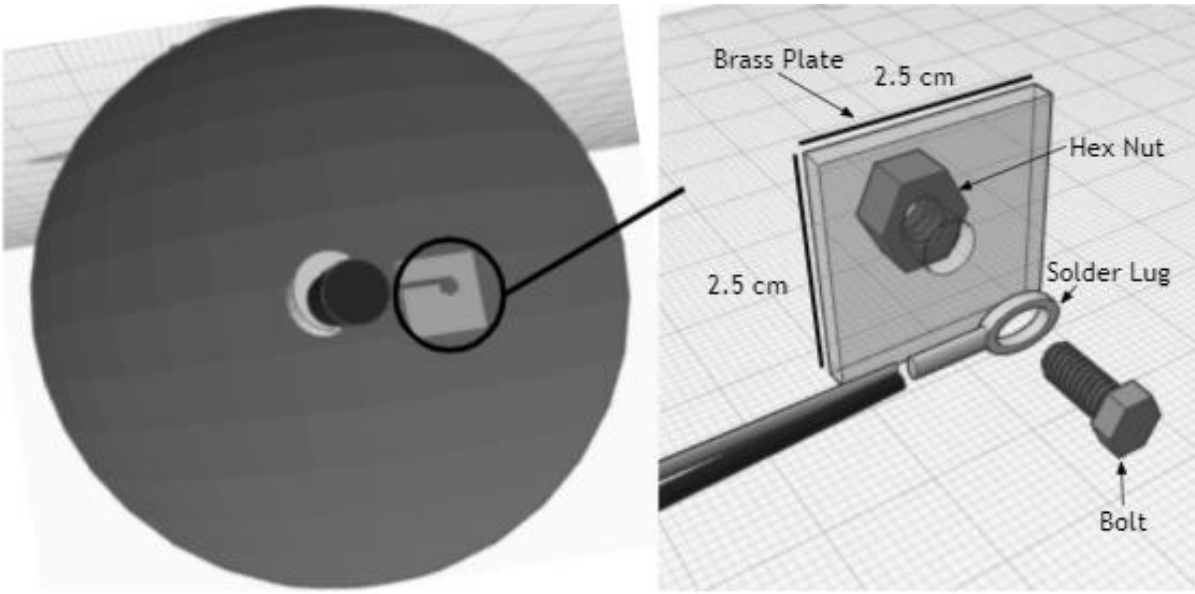

Figure 3: Model of probe plate assembly. The brass plate is electrically connected to the circuit that applies potential to the probe via a cable that runs through the boom shown in the center of the sphere. The sphere and probe plate are coated in Aquadag.

I hoped to use a 6 ft. carbon fiber tube as the boom to separate the probes. Carbon fiber is not only strong and lightweight, but also boasts high resistivity when woven so that fibers align transversely. High resistivity is a key requirement for a payload measuring such small electrical currents. However, while it was important to keep the payload down to a manageable size, the probes could not be too close together. With inadequate spacing, the conductivity measurements will contaminate each other, because the act of measuring temporarily changes the conductivity around each probe [19, 20]. To determine the minimum separation distance, the spherical probes can be approximated to point-like charges due to their symmetry. Therefore, the potential, Φ, of the sphere could be described by

$$\Phi = -\int \vec{E} \cdot \overrightarrow{dr} = \frac{q}{4\pi\epsilon_0 r}\,, \tag{3}$$

where E is the electric field, r is the radius of the sphere, and ϵ_0 is vacuum permittivity. The variable q is the charge that would collect on the sphere due to the applied potential. If a potential of +3 Volts is applied to a probe, the number of negatively charged particles, N, that would accumulate on the sphere can be calculated by

$$N = \frac{q}{e} = \frac{\Phi 4\pi\epsilon_0 \mathrm{r}}{\mathrm{e}} = 3.13\mathrm{x}10^8 \,, \tag{4}$$

assuming each particle has a charge of magnitude e equal to $1.6x10^{-19}$ C. Then, N is also equal to the number of positive ions in the surrounding air required to cancel out the excess charge. Using a typical ion density of 2 x 10^9 ions per m^3 [3], I calculated that the volume of a sheath of air needed to cancel out the point charge q would be V_s = 0.16 m^3. Accounting for the volume, V_p, of the probe itself, I calculated the approximate volume of air around the probe, V_{total}, that would be affected by the conductivity measurement to be

$$V_{total} = V_s + V_p = 0.121\, m^3 \,. \tag{5}$$

Therefore, the radius, R_{total}, of V_{total} is equal to 0.31 m. In my two-probe setup, the minimum separation distance, d_{min}, between the probes would be 0.62 m (illustrated in figure 4). Since the carbon fiber tube I intended to use was nearly 183 cm, I was able to proceed with confidence that the measurements would not contaminate each other.

4.2.2 Electrical Design

Figure 5 shows the block diagram for the electrical design. The two probes are electrically connected to the printed circuit board (PCB) via RG196 Teflon-insulated coaxial cable. Through these cables, the circuit can charge the probes to their opposite potentials. The “data” referred to on these cable lines in figure 5 is an analog signal from the probes, which will decrease as the potentials relax back to zero. The PCB amplifies this voltage and continuously feeds the signal to the microprocessor, providing the conductivity measurement data. Because the instrument will measure such a small current, very high impedance

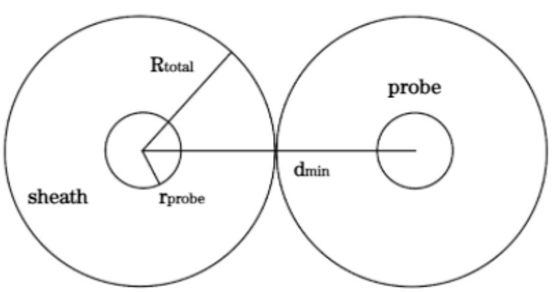

Figure 4: Illustration of the sheath of air surrounding the probes that would be affected by a measurement. The minimum separation distance, d_{min}, is equal to $2R_{total}$ and must be maintained to protect data quality.

on this circuit is critical. For this reason, the voltage on the probes cannot be measured directly by the microprocessor.

The microprocessor controls the timing of measurements, supplies voltage to the PCB and sensors, sends data to the interMet 4 RSB radiosonde (iMet), and runs the code that controls data conversion and storage. This design uses an Arduino Mega 2560 microprocessor due to cost and availability, but there are many suitable options.

The environmental sensors include the Adafruit LSM303AGR Accelerometer/Magnetometer; two DHT22 temperature-humidity sensors; an Adafruit LPS25 Pressure Sensor; and an Adafruit BME680 - Temperature, Humidity, Pressure and Gas Sensor. As shown in the sensor diagram in figure 6, some sensors are redundant and some are inside the payload box, while others are outside. The reason for this redundancy is that I want to see how each sensor performs on the instrument's maiden voyage, that way the design can be refined later to include the most effective sensors and arrangement. In addition to the environmental sensors, the payload will also include an Adafruit Ultimate GPS breakout board which

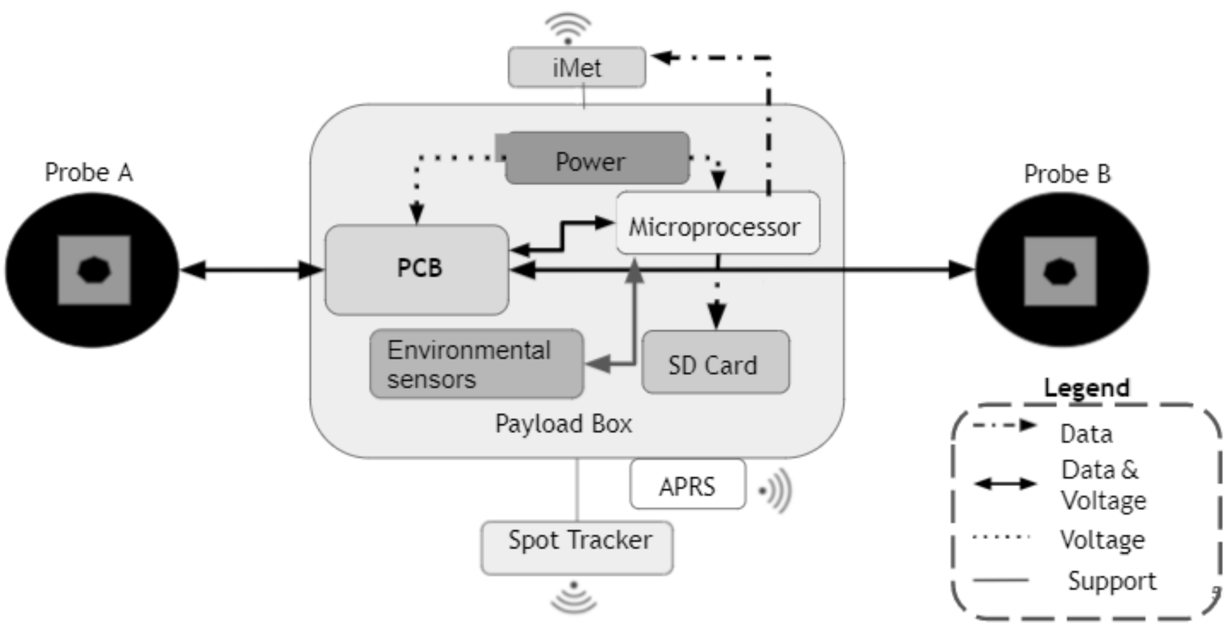

Figure 5: Block diagram for electrical design. This diagram shows electrical components of the payload, both inside and outside of the payload box. The iMet, Spot Tracker, and APRS systems communicate with the ground station during flight.

provides time and altitude information to the microprocessor. The iMet also contains a sensor suite to add another layer of redundancy should the other sensors prove unreliable.

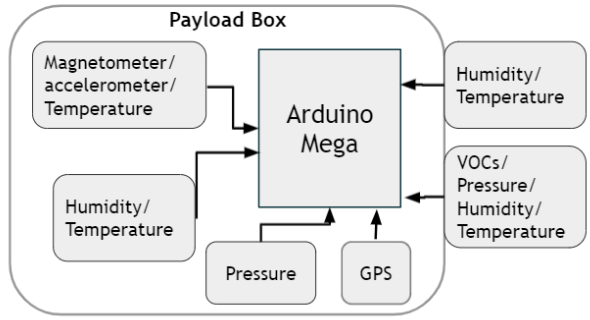

Figure 6: Sensor block diagram. Environmental information will be fed to the Arduino microprocessor from various sensors. The GPS breakout board will provide time and location information.

While the Arduino supplies power to the sensors and the multiplexer on the PCB, the Arduino itself is powered by a 9 V lithium battery. The operational amplifiers (op amps), and the reed relays on the PCB require their own power sources. Figure 7 contains the power diagram for the payload. The TL084 and AD549 op amps require +15 V and -15V supplies. To achieve this, a direct current to direct current (DC-DC) step-up converter amplifies the voltage from 9 V to 15 V. To create -15 V, a second converter is used backwards to reverse the sign on the voltage. The COTO reed relays used to drive the probes to potential use a 12 V supply for the coils. The 12 volts are provided by a set of two 9 V batteries placed in series, totaling 18 V. The voltage is then stepped down with another DC-DC converter. The 12 V potential drives a current through the coils of two

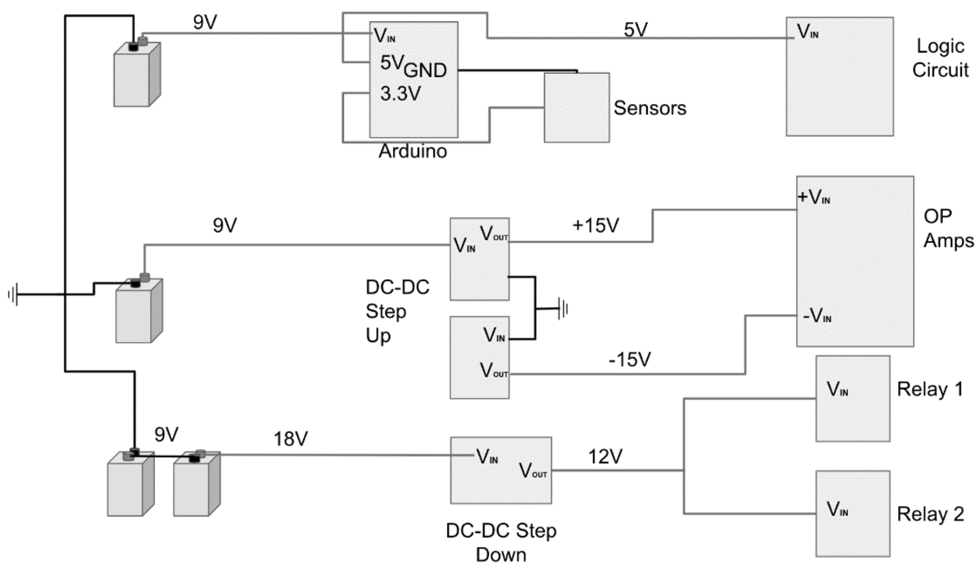

Figure 7: Power diagram for the payload. Four 9 V lithium-ion batteries serve as the voltage sources for the Arduino and PCB components. DC-DC converters are used to meet the specific voltage requirements of the operational amplifiers and reed relays.

reed relays, generating a magnetic field that causes a connection across the relays, allowing the desired potentials to be applied to the probes each measurement cycle.

Considerable time was devoted to selecting the best power system for this payload. Nickle-cadmium, alkaline, lead-acid, gel lead-acid, and lithium batteries were compared in trade studies. Lithium batteries emerged as the best choice because they are comparatively lightweight and have greater tolerance to the cold than other options. The choice of DC-DC converters was driven by weight considerations. The arrangement shown in figure 7 is lighter than options that use 12 V and 15 V batteries directly. In addition, 9 V lithium batteries are easier to acquire—especially in rechargeable varieties.

4.2.3 Software

One benefit of using an Arduino microcontroller in the design was that the complexity of the PCB could be reduced dramatically compared to the circuit it was based on. Several functions that were previously completed on the board can be performed by the Arduino, such as the measurement cycle timing. A *measurement cycle* here is defined as one cycle of grounding the probes for two seconds to verify the zero-level, two seconds of charging the probes to potential (one positive, one negative), then releasing the relays and allowing time for the potentials to relax. When the next measurement cycle begins, the signs of the potentials will be reversed. *Sampling* is defined here as the Arduino recording a measurement of the voltage of each probe. With this terminology then, the Arduino will *sample* the voltage at some frequency throughout a *measurement cycle*. Therefore, there is a sampling frequency, and a separate measurement cycle frequency, with the sampling frequency always much higher than the measurement frequency.

Based on past research, I expect a conductivity, $\sigma_{0,}$ of about 10^{-13} $(\Omega \cdot m)^{-1}$ near the surface of the Earth [15]. At the maximum expected height, the conductivity, σ(z=32), should be close to 10^{-11} $(\Omega \cdot m)^{-1}$. In between, the conductivity should increase exponentially according to the function

$$\sigma(z) = \sigma_0 \exp(z/h) \,, \tag{6}$$

where σ_0 is a reference conductivity (that is, the conductivity at ground level), z is the altitude above mean sea level, and h is the conductivity scale height [16, 7]. The boundary conditions at $z = 0$ and $z = 32$ were used to calculate the scale height. However, to build an equation that aligned with previous research data a piecewise function was ideal (Shown in figure 8). The need for a piecewise function, breaking around the tropopause, is consistent with previous studies [7, 15]. From 0 to 20 km, a scale height of 6 was used in the equation shown in figure 8, and 7 was used for higher altitudes.

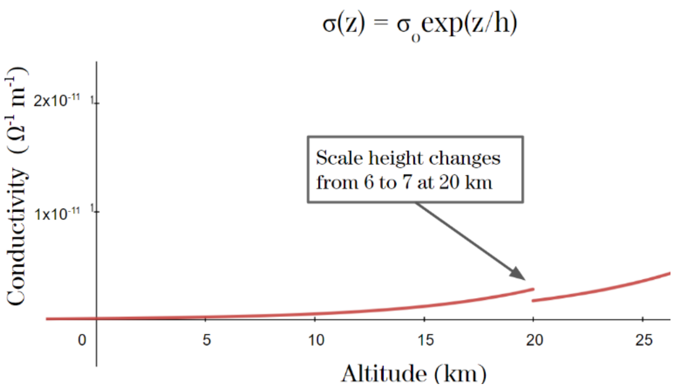

Figure 6: The theoretical conductivity as a piecewise function. The conductivity is expected to increase roughly according to $\sigma(z) = \sigma_0 \exp(z/h)$, with the scale height h changing around 20 km.

Since there is such a difference in the conductivity at 0 and 32 km, it is ideal to vary the timing of the measurement cycle according to altitude. Otherwise, there will be sections of the flight where data is either unusable, or too sparse. If the measurement frequency is too high, data at low altitudes will be useless since the potentials will not have enough time to relax between measurements. If it is too slow, then interesting data at high altitudes will be lost because the probe potentials will be fully relaxed most of the time between measurements. Therefore, the measurement cycle frequency should vary as the time constant of the decay varies. Since $\sigma = \epsilon_0/\tau$, the time constant can be expressed as a function of altitude, z, by

$$\tau(z) = \frac{\epsilon_0}{\sigma_0 \exp(z/h)} \,, \tag{7}$$

where again, the scale height, h, is 6 at $z < 20$ km, and 7 at $z > 20$ km. The time, *t,* between the measurement cycles needs to exceed the time constant to allow full relaxation. Therefore, the equation used in the Arduino code to determine the time between measurement cycles was

$$t(z) = \frac{10\epsilon_0}{\sigma_0 \exp(z/h)}. \tag{8}$$

In the Arduino code, written by Andy Nguyencuu, a master loop will regulate timing, measurement cycle calculation, and recovery in case of failure. Subroutines will regularly perform sensor measurements, data collection, and error checking. The measurement cycle frequency will constantly update as GPS altitude is updated by the Ultimate GPS board. The voltage values from the probes will be relayed by the PCB to the AD2499 Analog to Digital Converter shield. There, it will be digitized, then sent by the Arduino to the iMet in XDATA format. Fine data and timestamps will be written to an onboard SD card, but recovering this data requires tracking the payload's landing and successfully recovering it. The iMet will transmit the data in-flight to the ground as a radio signal so that live data can be recorded. That way, even if payload recovery is not possible, all data is not lost. The iMet will also transmit its own suite of atmospheric sensor data and GPS to add another layer of redundancy. Still, the iMet requires line-of-sight for transmission so there are many obstacles that can impede transmission. Evaluation of the raw data will be done on the ground.

4.2.4 Payload Box

The payload is expected to reach an altitude of 30 to 32 km, taking data throughout the entire flight. As such, the electronics will be subject to extreme temperatures, low pressure, and sudden impact at a velocity of approximately 5 m/s. It was therefore essential to design an insulated payload box that could house the electronics securely, while maintaining low weight. The material chosen for this job was 2-inch polystyrene foam board, used for housing and

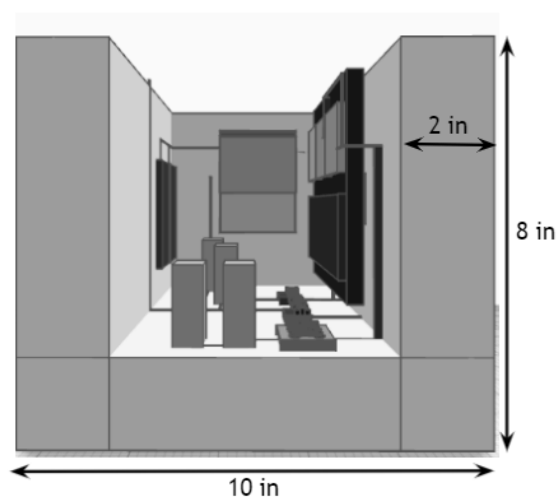

Figure 7: Model of the payload box and interior components. The lid is not shown in this cross section of the box.

recreational vehicle insulation. These boards can be cut with relative ease and assembled using RTV 102 glue which performs well at low temperatures. To provide additional security and insulation, the corners of the payload box would be sealed using 100% silicone caulk. The interior box dimensions were kept as small as was practical to reduce weight and help with insulation (shown in figure 9). The box would be attached to a Polyvinyl chloride (PVC) support cross above it with monofilament (fishing line). The support cross connects the box to the rest of the flight train.

On the exterior of the box, I added Aquadag-coated aluminum plates to the design on the advice of Dr. Bering. These provide a grounding surface for the electronics as well as for the grounding cables that would be connected to the probes until just before launch. The grounding cables are necessary to keep the instrument "off" until ready to launch, and to protect the preamps on the circuit. Furthermore, since the payload box would be difficult to handle once the coated grounding plates have been added (since they cannot be touched), "feet" were added to the bottom of the box in the form of 4 short pieces of PVC pipe. The feet not only provide a surface to grab onto, but they also keep the payload cleaner by elevating it off the ground during flight preparations.

Attached to the exterior structure of the box and PVC support cross, we added the telemetry and navigation equipment to the design. A triple-redundant tracking system would be used to increase the chance of payload recovery, including a SPOT tracker, an Automatic Packet Reporting System (APRS), and the iMet. As discussed previously, in addition to providing a GPS location, the iMet would send the telemetry to the ground station during flight in case retrieval of the onboard SD card was not possible. The iMet radiosondes are designed specifically for balloon flights and are used regularly by other research projects. As such, they were a reliable choice for USIP balloon instruments; however, they can still fail, and they require line-of-sight for communication, so they often provide no tracking information in the late stages of a flight. The SPOT Tracker is a durable safety tracker geared towards exploring and hiking. It has tracking functionality that uploads its location to satellites. The drawback of the SPOT is that they typically deactivate over 60,000 ft. There is about a 50/50 chance of reactivation during descent so it may be useless for most of the flight, but it was deemed to be worth including. The APRS is a small circuit board with antennas that transmits GPS information periodically, through repeater stations, to an internet gate (iGate) that uploads that data to APRS servers. The APRS should be able to transmit location as long as there are amateur radio repeater stations within range below the balloon.

4.3 Cleanliness and Encapsulation

The design description for this payload would not be complete without mentioning the need for cleanliness and encapsulation. The ions moving through the air, in response to the applied probe potential, comprise a very small current. If even small amounts of current are diverted from the path shown in figure 10, the measurement will be severely degraded. It is therefore critical that all exterior materials (except for the probes and grounding plates) in this design are high impedance and are kept clean. Additionally, areas that are likely to "leak" current, particularly on the circuit board, need to be encapsulated. Consider that the measurement being made is so precise that a fingerprint on the circuit board can affect the results.

The first requirement was addressed with the woven carbon fiber tube, and the foam payload box materials that were chosen. Additionally, a payout reel was added to the flight train to provide 100 ft. of separation between the balloon and the instrument so that there is no chance of the balloon contaminating the measurement. To enhance the resistivity of all exposed materials, excluding the grounding plates,

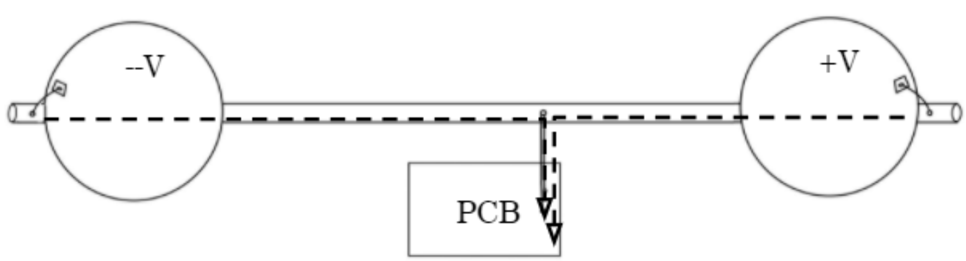

Figure 8: Path of current from the probes. Current will flow between the probes and the PCB, allowing the Arduino to sample the probe potentials as they decay.

probes, and payload box foam, a five-step cleaning process was planned for. Before final assembly, the cables, boom (inside and out), and the circuit board, including components, need to be washed in the following process:

1. Use a soap and tap water solution with a rag or cotton ball to wash the parts.
2. Rinse all pieces with deionized water. This and the subsequent steps may be done using a squeeze bottle.
3. Heat with hair dryer.
4. Wash pieces with reagent grade ethanol.
5. (Optional) wash with methyl ethyl ketone if much soldering has taken place.
6. Wash all components with acetone.
7. Wash the components in freon TF.

All this washing is done in the lab after any cutting, drilling, sanding, soldering, etc. has been completed. The process may need to be repeated after transporting to a launch location. The high impedance of the payload components is so important that it is even necessary to wash the coax cable ends that connect to the brass probe plates before encapsulating them with heat shrink tubing, as illustrated in figure 11. While in the field just before a launch, the outside of booms and cables should be washed with ethanol and freon once more.

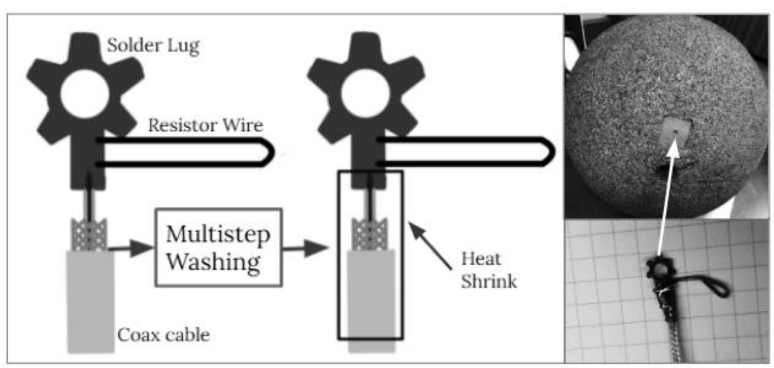

Figure 9: Coaxial cable ends. The ends of the coax cable that connect to the probes is diagramed here. The multistep washing process must be performed before the cable ends are sealed with heat shrink.

On the circuit board, the primary areas of concern were the areas where the preamplifiers and the relays are located. Consequently, the use of copper zones was employed (visible as blue rectangles on the board layout image in Appendix A). Rectangular brass covers would be soldered overtop the zones to completely encapsulate these regions of the board with a surface that has a potential equal to the ambient potential of the air around the probes. Furthermore, RTV 102 would be used to pot this section of the board.

5 Results

The product of the design phase is depicted in figures 12 and 13. This balloon payload, consisting of two spherical probes was designed to weigh less than 2.72 kg and achieve a height of approximately 32 km before the latex weather balloon bursts. The atmospheric conductivity will be measured using the relaxation time method where the two probes will be charged to opposite potentials. When released, the potentials will decay exponentially by movement of ions through the air around the probes. The conductivity measurement will be achieved by determining the time constant of the decay. At the start of each measurement cycle, the probe potentials will be reversed; in other words, the probe that was +3 V on the previous cycle will be –3 V on the following cycle. The reversal of the polarity each time guards against systematic errors. A triple-redundant tracking system included in the design will be used to increase the chance of payload recovery. Data will also be transmitted during the flight in case retrieval of the onboard SD card is not possible.

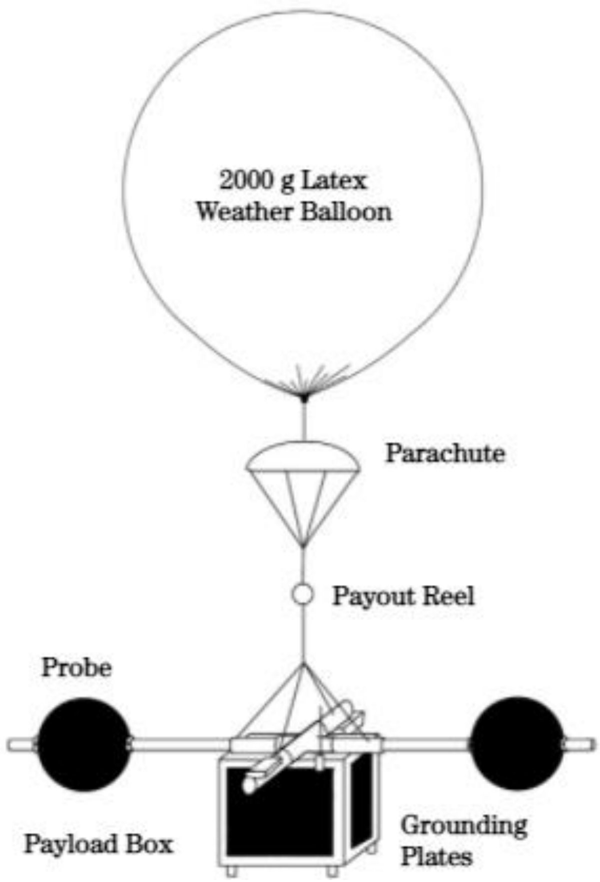

Figure 10: Payload design outline with flight train. Two probes are connected to electronics housed in the payload box to carry out conductivity measurements via the relaxation time method.

To test the design, a prototype was constructed. The construction phase began January 2021 and continued through the writing of this

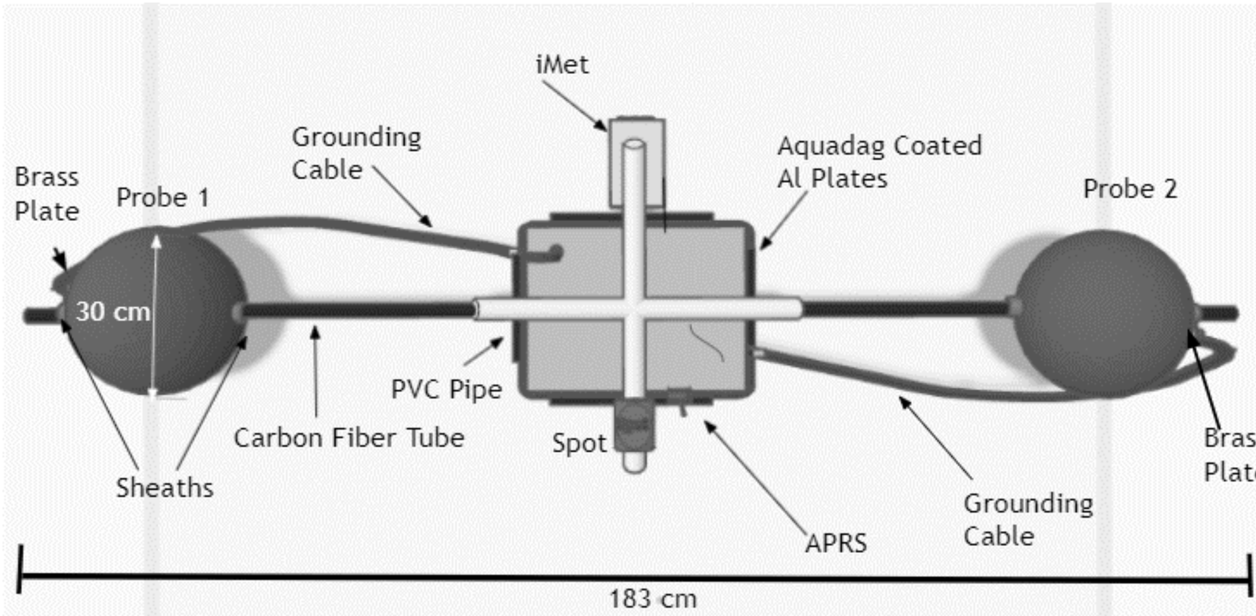

Figure 11: Top view of conductivity payload model. Temporary grounding cables are intended to be removed before flight. Sheaths on either side of probes prevent movement along the boom. Spot, and iMet tracking systems are attached to the support cross. The APRS is fixed vertically on the side of the box.

thesis. Appendix B provides a complete list of materials used to build one payload in addition to the balloon, helium, parachute, and payout reel. Spare parts are not included in these lists but are recommended with a healthy appreciation for Murphy's Law.

To make the probes, a 5:1 water to Aquadag ratio was used and six-to-eight thin coats per sphere were required. Thin coats are desirable to prevent flaking. The small brass plate was glued on and pressed into the probe slightly after one coat of Aquadag. On the next coating of the probe, a hair dryer was used on just the plate, otherwise, the Aquadag would not adhere to the brass. The same solution of Aquadag was used for several days to avoid waste.

I was skeptical that an applied potential would evenly distribute across the probe surface as was assumed in earlier calculations. Therefore, once the probes, cables, and boom had been assembled, the probe spheres were tested by connecting the circuit end of the cable to a power supply. A digital multimeter (DMM) was used to probe the surface of the sphere at six different points across the probe to see if it was charging to the expected potential. Table 1 displays the results of one test, showing that the

Table 1: Probe testing results. Supplied potential was compared to measured potentials to check for even distribution across the probe. The measurement error is +/- 0.04 V.

DMM Probe Position	Supplied Potential (V)	Measured Potential (V)
A	3.01	3.02
B	3.01	3.02
C	3.01	3.02
D	3.01	3.02
E	3.01	3.01
F	3.01	3.02

potential was approximately equal at every point measured. Further testing on the probes is required but these preliminary measurements are reassuring. The conductive coating on the spheres, and design of the cables are effective.

Initial tests with the Arduino, connected to the sensors and GPS board, confirmed that the code was working, and all sensors were reporting values. However, the DHT22 temperature-humidity sensors consistently reported temperatures and humidity percentages that disagreed dramatically with the other sensors. Thus far, the DHT22 sensors do not seem to be reliable despite manufacturer reported accuracy of +/-0.5˚C and +/-5% humidity. Figure 14 shows the two LPS25 (accuracy +/-1 hPa) sensors and the BME680 (accuracy +/-1˚C and +/-1 hPa) test results compared to a Kestrel Weather Meter (accuracy +/-

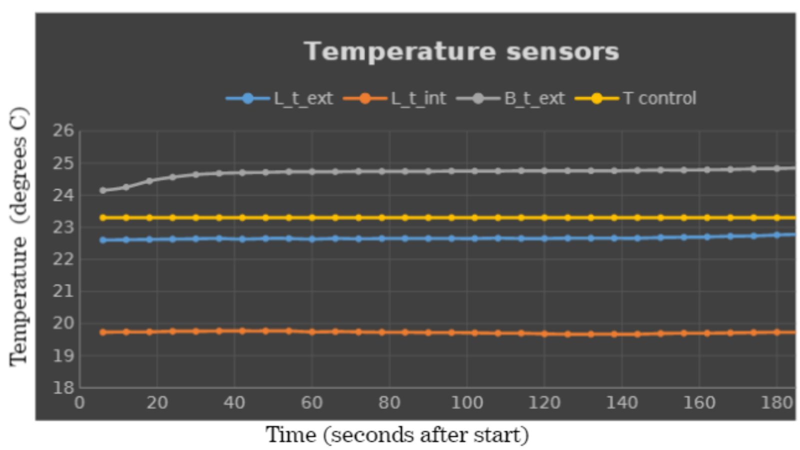

Figure 12: Temperature sensor comparison. L_t_ext is the LPS25 that will be used externally, L_t_int is the LPS25 that will be inside the payload box. B_t_ext is the BME680. T control is the Kestrel Weather Meter.

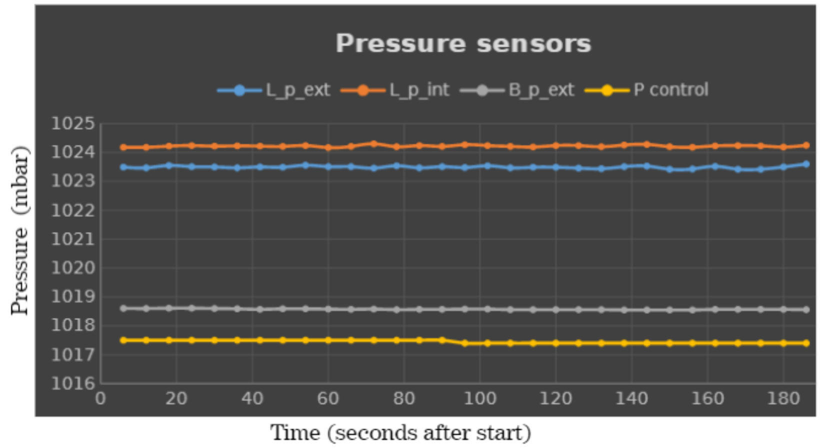

Figure 13: Pressure sensor comparison. L_p_ext is the LPS25 that will be used externally, L_p_int is the LPS25 that will be inside the payload box. B_p_ext is the BME680. P control is the Kestrel Weather Meter.

0.5˚C and +/-1 hPa) that is used regularly as a control in the Ozone laboratory at University of Houston. During the same ambient-air laboratory test, the pressure values were also recorded for these four sensors. Those values are shown in figure 15.

The complete board layout and schematic can be found in Appendices A and C, respectively. The circuit design passed all design rule, netlist, and connectivity checks in Multisim and Ultiboard. The +12 V supply to the relays was tested on a small breadboard circuit because the relays were updated from previous designs. The older design contained now-obsolete relays that required a +28 V supply. Some resistor values also needed to be updated, but the breadboard testing confirmed that the relays will function properly in the new design.

Structural testing of the prototype has shown that the durability of the payload box is satisfactory. Through drop tests (payload box is dropped from varying heights with weight inside), roll tests (weighted box is rolled down stairs), and whip tests (weighted payload is attached to support cross and spun around), the prototype boxes were shown to withstand stress and strain similar to a balloon flight. While damage to the payload structure is expected upon landing, the stored data should be recoverable, and the payload box is not considered to be at risk for damage during the flight.

Keeping the electronics warm in the payload box is another matter. At high altitudes, temperatures can reach –70 ˚C or lower. Tests conducted in the laboratory at –60 ˚C showed significant risk of electrical failure at high altitudes. Several heating methods were explored, including electronic heating pads, chemical hand warmers, internal fans with hand warmers, and hot water bottles. Weight and battery power were the limiting factors, and so chemical hand warmers will be fixed to the inside of the payload box, and further attention will be devoted to insulating the box before launch.

To increase the shareability of the design, I created a website where I can upload all necessary design specifications, pictures, notes, and parts lists. ConductivityResearch.com will be an evolving product of this thesis that has the potential to be continually useful long after the printed copy is produced. If new iterations of the design are created, new parts made available, or information is otherwise updated, the new information can be added to the site, allowing it to be shared instantly, worldwide.

6 Discussion

The primary goal of this thesis was to provide and describe a design for a low-cost, lightweight instrument that can measure stratospheric conductivity. This goal was met with a payload design based on tried-and-true methods of measurement with modifications to decrease the weight and cost factors dramatically. The payload prototype weighs 2.72 kg, not including the flight train and telemetry/navigation equipment. The payload plus the flight train will weigh less than the 5.44 kg (12 lb.) maximum set by the FAA and can be carried by a 2000 g weather balloon with limited regulation.

The secondary objective was to assess the feasibility for replication of the instrument by other college or high school students. To start, the design met cost requirements. A single copy of this instrument cost approximately $1,500. The total cost was just under $2,000 including the balloon, helium, and flight train—well within the $3000 budget. However, it is important to consider that this total does not include any spare parts, so actual costs will be higher depending on how many extra items are purchased. Communication and tracking equipment for the ground station were excluded as well since that cost is highly dependent on whether a group already conducts any kind of similar research. And there will, of course, be variability in the cost over time; however, this value of $2,000 sets a general expectation of the budget that will be required to undertake this experimental research.

Concerning complexity, this design requires very few materials that cannot be found through popular distributors. Items that are more difficult to find, such as Aquadag, will be listed on the website with links to manufacturers or distributors where they have been found previously. Beyond parts acquisition, the payload is relatively simple to construct, requiring no more specialized equipment than a drill press. The circuit board must be printed by professionals, but the Gerber files, .pdf, .ms14 (Multisim file format), and .ewprj (Ultiboard file format) files will be uploaded to the website so that they can be easily replicated, modified, or just sent straight to a local board house.

Aspects of this experiment are likely to change over time and ConductivityResearch.com gives it flexibility. For example, the code to run all payload operations, including charging the probes, sampling the voltages, sampling the sensor data, and transmitting XDATA has been drafted. The code is functional; however, it will continue to be modified leading up to a, and likely after, the flight of this instrument. Therefore, the code versions will be made available on the website as the project continues. The addition of the website to the results of this thesis increases the likelihood that this experiment will be repeated by others since the design has already been completed and the details shared on the internet. This thesis may even lead to the development of an experimental kit that can be sold online to further decrease barriers to stratospheric conductivity research.

Although the primary goals of this thesis have been met, the prototype of the payload has yet to be flown and there are many tests that still need to be performed prior to launch. Environmental sensor testing results show significant disagreement between sensors. The LPS25 that is intended to be mounted on the exterior of the payload box read closest to the control temperature during the three-minute test, but the BME680 was closest in pressure. Tests such as these need to be repeated under a variety of conditions, including vacuum conditions. Physical testing and calibration of the circuit board is also essential before flight. There is much that can be done to increase the chances of success on the instrument's maiden voyage. Therefore, the work will continue; and the website ensures that improvements, additions, and experimental results can be shared easily.

7 Conclusion

To better understand the global electric circuit, hundreds of measurements of atmospheric conductivity were made around the world. However, these efforts have not provided enough information to construct an accurate global model. The design created for this thesis—weighing 2.72 kg and costing about $2,000—can be used to add new stratospheric conductivity measurements to the global dataset and explore possible causes of the short-term variance, among other things.

To contribute directly to this goal, future work is already planned as the USIP IV program continues into 2022. Data collection with instruments following the design outlined in this thesis is planned to occur in two balloon campaigns--each at a different latitude. The first payload will launch in Texas in late 2021 at approximately 30 degrees North. The second flight will take place at a latitude of approximately 65 degrees North in Alaska in 2022. A conductivity latitude gradient is expected to be observed because the Earth's magnetic field offers more shielding from cosmic rays near the equator that it does at the poles. Therefore, conductivity is expected to be higher in the polar regions, as observed in previous research. During data analysis, the conductivity measurements will be compared to the results of other USIP IV experiments conducted during the same campaign. The other teams will measure airborne microplastics, energies of precipitating auroral electrons, very low frequency (VLF) waves, and gaseous compounds including CO, NO, NO_2, H_2S, SO_2, and O_3. To make the comparisons between these measurements and the conductivity, the payloads will be launched close together, in time and space. The timestamped data collected by the other experiments will be compared to the conductivity data to see if any correlations can be observed, and the results of these flights can be uploaded to the ConductivityReasearch.com to continue adding value to this thesis.

Appendix A

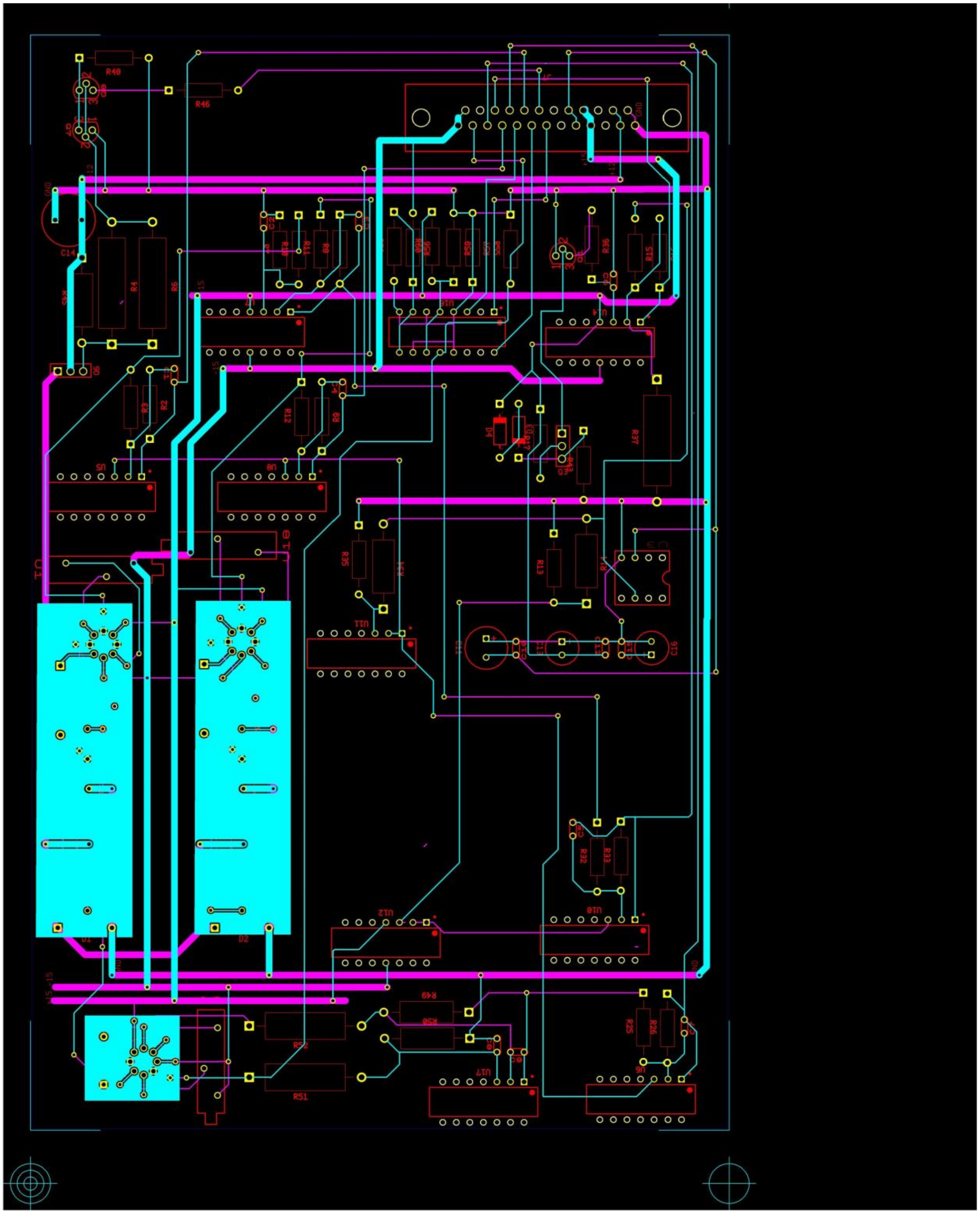

Figure A: Board layout of conductivity PCB. Copper top is shown in purple. Copper bottom is shown in blue.

Appendix B

Table B: List of all items, including quantity and cost, used to construct the payload prototype.

Item	**quantity for one payload (no spares)**	**cost per item**	**total cost**
Resistors (Ohms)			
1.2kOhm 1%	2	$0.26	$0.52
1GOhm	1	$6.34	$6.34
4kOhm 1%	1	$0.29	$0.29
5.3kOhm	1	$1.50	$1.50
5kOhm 1%	1	$0.29	$0.29
5kOhm 1%	2	$0.29	$0.58
10kOhm	5	$0.10	$0.50
10kOhm 0.01%	3	$6.30	$18.90
10kOhm 1%	5	$0.10	$0.50
10kOhm 1%	1	$0.10	$0.10
20kOhm .01%	1	$6.00	$6.00
22MOhm	2	$0.65	$1.30
24kOhm 1%	1	$0.05	$0.05
25kOhm .01%	2	$10.00	$20.00
33kOhm	1	$0.18	$0.18
51kOhm 1%	1	$0.40	$0.40
60.4KOhm 1%	1	$0.12	$0.12
60.4kOhm 1%	1	$0.12	$0.12
60kOhm 1%	1	$1.34	$1.34
68.1kOhm 1%	1	$1.00	$1.00
72kOhm 1%	2	$1.00	$2.00
84.5kOhm 1%	1	$1.00	$1.00
100kOhm	1	$2.08	$2.08
510Ohm	1	$0.99	$0.99
Variable Resistor	3	$3.00	$9.00

Capacitors/Diodes			
0.1 muF Ceramic	9	$0.63	$5.67
0.1 muF Aluminum Electrolytic	3	$0.17	$0.51
0.001 muF Ceramic	1	$0.50	$0.50
100 muF Aluminum Electrolytic	2	$1.19	$2.38
330 muF Ceramic	1	$0.31	$0.31
78 muF Aluminum Electrolytic	1	$4.00	$4.00
1N914 Diode	3	$0.10	$0.30
Diode ZE 6.8V Zener	1	$0.17	$0.17
Amps/Transistors			
TL084CN Op Amp	9	$0.42	$3.74
74HC74 Logic IC	1	$0.55	$0.55
AD549 Op Amp	3	$57.06	$171.18
2N4918 PNP	1	$0.66	$0.66
2N3565 NPN	2	$2.98	$5.96
2N5139 PNP	1	$2.98	$2.98
MTS 102 601K NPN	1	$10.66	$10.66
Relays			
COTO 1240-0255	2	$35.36	$70.72
Structural Material			
Styrofoam sheets R-7.8 2-in x 4-ft x 8-ft	2	$20.98	$41.96
RTV 102 White 10.3 fl. oz.	1	$34.62	$34.62
Fiberglass Tape	1	$8.88	$8.88
PVC Pipe (10 ft.)	1	$3.64	$3.64
PVC Cross Junctions	1	$2.62	$2.62
Batteries			
9V Energizer Battery	4	$10.98	$43.92
Battery Clips	1	$5.59	$5.59
Converters			
Step Down Converter	1	$2.35	$2.35
Step up Converter	2	$1.50	$3.00

Telemetry/navigation			
iMet 4 RSB	1	$225.00	$225.00
SPOT Gen4	1	$149.99	$149.99
SPOT Flex (monthly) service plan	1	$14.95	$14.95
GPS Antenna - External Active Antenna - 3-5V 28dB 5 Meter SMA	1	$17.95	$17.95
Sensors			
DHT22 temperature-humidity sensor	2	$9.95	$19.90
Adafruit BME680 - Temperature, Humidity, Pressure and Gas Sensor - STEMMA QT	1	$18.95	$18.95
SD card	1	$9.95	$9.95
LSM303AGR ACCEL MAG STEMMA QWIIC	2	$8.95	$17.90
LPS25 PRESSURE STEMMA QT / QWIIC	2	$5.95	$11.90
Ultimate GPS Breakout Board	1	$29.95	$29.95
Avionics			
DATA LOGGING SHIELD	1	$13.95	$13.95
Arduino Mega	1	$40.00	$40.00
2499 ADC shield	1	$55.00	$55.00
Shield stacking headers	1	$1.76	$1.76
Flight Train			
2000g weather balloon, latex	1	$250.00	$250.00
Monofilament fishing line spool	1	$32.00	$32.00
Payout reel	1	$25.00	$25.00
8ft parachute	1	$75.00	$75.00
Zip ties with eyelets	1	$6.70	$6.70
Helium	1	$100.00	$100.00
6 ft. Carbon fiber tube (3/4 inch diameter)	1	$120.00	$120.00
Aquadag	1	$40.00	$40.00
Sheet Aluminum (3ft x 3ft)	1	$50.00	$50.00
PCB Printing	1	$100.00	$100.00
Shorting Plug	1	$5.00	$5.00
RG196 Teflon-insulated coaxial cable (1ft)	10	$1.70	$17.00

Foam Sphere	2	$9.00	$18.00
Total Cost			**$1,967.83**

Appendix C

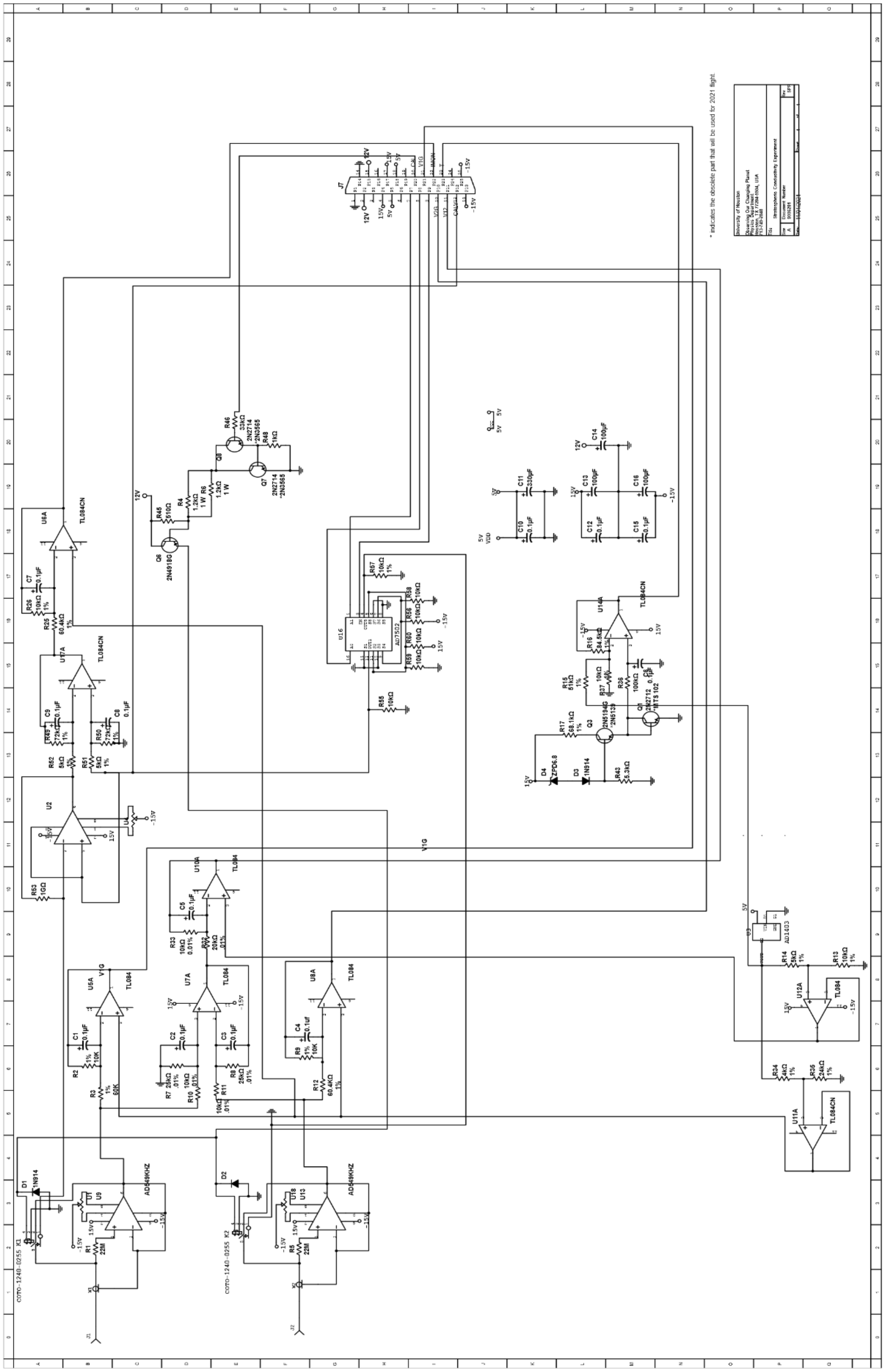

Figure C: Conductivity PCB Schematic

BIBLIOGRAPHY

[1] Byrne, G. J., Benbrook, J. R., and Bering, E. A. "Balloon Observations of Stratospheric Electricity above the South Pole: Vertical Electric Field, Conductivity, and Conduction Current." *Journal of Atmospheric and Terrestrial Physics*, Vol. 53, No. 9, 1991, pp. 859–868.

[2] G. Baumgaertner, A. J., Thayer, J. P., Neely, R. R., and Lucas, G. "Toward a Comprehensive Global Electric Circuit Model: Atmospheric Conductivity and Its Variability in CESM1(WACCM) Model Simulations: MODEL SIMULATIONS OF GEC CONDUCTIVITY." *Journal of Geophysical Research: Atmospheres*, Vol. 118, No. 16, 2013, pp. 9221–9232.

[3] Bering, E. A., Benbrook, J. R., Holzworth, R. H., Byrne, G. J., and Gupta, S. P. "Latitude Gradients in the Natural Variance in Stratospheric Conductivity – Implications for Studies of Long-Term Changes." *Advances in Space Research*, Vol. 35, No. 8, 2005, pp. 1385–1397.

[4] Byrne, G. J., Benbrook, J. R., Bering, E. A., Oró, D., Seubert, C. O., and Sheldon, W. R. "Observations of the Stratospheric Conductivity and Its Variation at Three Latitudes." *Journal of Geophysical Research*, Vol. 93, No. D4, 1988, pp. 3879–3891.

[5] Dhanorkar, S., and Kamra, A. K. "Calculation of Electrical Conductivity from Ion-Aerosol Balance Equations." *Journal of Geophysical Research: Atmospheres*, Vol. 102, No. D25, 1997, pp. 30147–30159.

[6] Pan, B., Wang, Y., Logan, T., Hsieh, J., Jiang, J. H., Li, Y., and Zhang, R. "Determinant Role of Aerosols From Industrial Sources in Hurricane Harvey's Catastrophe." *Geophysical Research Letters*, Vol. 47, No. 23, 2020, p. 10.

[7] Bering, E. A., Benbrook, J. R., Byrne, G. J., Holzworth, R., and Gupta, S. P. "Long Term Changes in the Electrical Conductivity of the Stratosphere." *Advances in Space Research*, Vol. 32, No. 9, 2003, pp. 1725–1735.

[8] Deshpande, C. G., and Kamra, A. K. "Atmospheric Electric Conductivity Measurements over the Indian Ocean during the Indian Antarctic Expedition in 1996-1997: ELECTRIC CONDUCTIVITY." *Journal of Geophysical Research: Atmospheres*, Vol. 107, No. D21, 2002, pp. ACH 14-1-ACH 14-9.

[9] Mosayebidorcheh, T. "Analytical Solution of Electromagnetic Radiation by a Vertical Electric Dipole inside the Earth and the Effect of Atmospheric Electrical Conductivity Inhomogeneity." *Advances in Space Research*, Vol. 60, No. 9, 2017, pp. 1949-1957.

[10] Samimi, A., and Simpson, J. J. "An Efficient 3-D FDTD Model of Electromagnetic Wave Propagation in Magnetized Plasma." *IEEE Transactions on Antennas and Propagation*, Vol. 63, No. 1, 2015, pp. 269–279.

[11] Adach, S., Yasukawa, H., Takumi, L., and Hata, M. "Signal Processing and Sonification of Seismic Electromagnetic Radiation in the ELF Band." *IEICE Transactions on Fundamentals of Electronics, Communications and Computer Sciences*, Vols. E84-A (4), 2001, pp. 1011–1016.

[12] Alperovich, L., and Fedorov, E. “Perturbation of Atmospheric Conductivity as a Cause of the Seismoionospheric Interaction.” *Physics and Chemistry of the Earth*, Vol. 23, Nos. 9–10, 1998, pp. 945–947.

[13] Heaps, M. G. “Parameterization of the Cosmic Ray Ion-Pair Production Rate above 18km.” *Planetary and Space Science*, Vol. 26, 1978, pp. 513–517.

[14] Bering, E., Engebretson, M., Holzworth, R., Kadokura, A., Kokorowski, M., Reddell, B., Posch, J., and Yamagishi, H. “Simultaneous Observations of Pc 1 Micropulsation Activity and Stratospheric Electrodynamic Perturbations on 27 January 2003.” *Advances in Space Research*, Vol. 43, No. 5, 2009, pp. 802–818.

[15] Bering, E. A., Holzworth, R. H., Reddell, B. D., Kokorowski, M. F., Kadokura, A., Yamagishi, H., Sato, N., Ejiri, M., Hirosawa, H., Yamagami, T., Torii, S., Tohyama, F., Nakagawa, M., and Okada, T. “Balloon Observations of Temporal and Spatial Fluctuations in Stratospheric Conductivity.” *Advances in Space Research*, Vol. 35, No. 8, 2005, pp. 1434–1449.

[16] Holzworth, R. H. “Conductivity and Electric Field Variations with Altitude in the Stratosphere.” *Journal of Geophysical Research*, Vol. 96, No. D7, 1991, pp. 12857-12864.

[17] Byrne, G. J., Benbrook, J. R., Bering, E. A., and Oró, D. M. “Solar Radiation (190–230 Nm) in the Stratosphere: Implications for Photoelectric Emissions from Instrumentation at Balloon Altitudes.” *Journal of Geophysical Research*, Vol. 95, No. D5, 1990, pp. 5557–5566.

[18] Mozer, F. S., and Serlin, R. “Magnetospheric Electric Field Measurements with Balloons.” *Journal of Geophysical Research*, Vol. 74, No. 19, 1969, pp. 4739–4754.

[19] Fahleson, U. “Theory of Electric Field Measurements Conducted in the Magnetosphere with Electric Probes.” *Space Science Reviews*, Vol. 7, Nos. 2–3, 1967, pp. 238–262.

[20] Chang, J.-S., and Kodera, K. “Theory of Electric Conductivity Measurements by an Electrostatic Probe in an Atmospheric Low-Density Continuum Ionized Gas.” *Journal of Geophysical Research*, Vol. 90, No. D4, 1985, pp. 5897–5900.